ChemComm

Accepted Manuscript

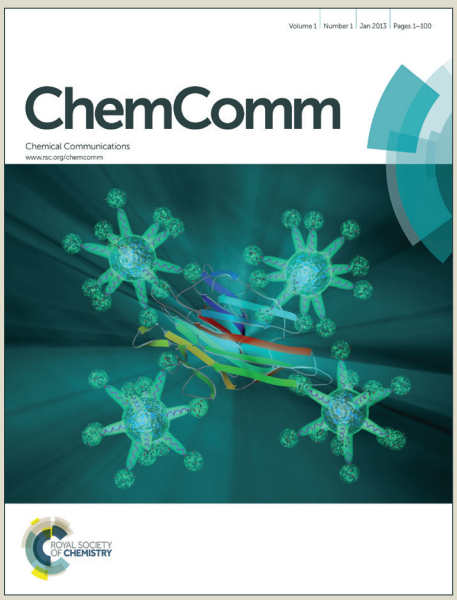

This is an *Accepted Manuscript*, which has been through the Royal Society of Chemistry peer review process and has been accepted for publication.

Accepted Manuscripts are published online shortly after acceptance, before technical editing, formatting and proof reading. Using this free service, authors can make their results available to the community, in citable form, before we publish the edited article. We will replace this *Accepted Manuscript* with the edited and formatted *Advance Article* as soon as it is available.

You can find more information about *Accepted Manuscripts* in the Information for Authors.

Please note that technical editing may introduce minor changes to the text and/or graphics, which may alter content. The journal's standard Terms & Conditions and the Ethical guidelines still apply. In no event shall the Royal Society of Chemistry be held responsible for any errors or omissions in this *Accepted Manuscript* or any consequences arising from the use of any information it contains.

ROYAL SOCIETY OF CHEMISTRY

www.rsc.org/chemcomm

Journal Name RSCPublishing

COMMUNICATION

High-yield electro-oxidative preparation of graphene oxide

Cite this: DOI: 10.1039/x0xx00000x

A. M. Abdelkader,[a,b] I. A. Kinloch [a] and R. A. W. Dryfe[a,b]

Received 00th January 2012,
Accepted 00th January 2012

DOI: 10.1039/x0xx00000x

www.rsc.org/

Herein, we report a green electrochemical oxidative approach to convert large quantities of graphite into graphene oxide (GO). The resulted GO flakes have been characterized using various analytical techniques. It was possible to control the degree of oxidation of the produced GO via controlling the electrochemical parameters of the process.

Graphene, a single two-dimensional layer of carbon atoms, and its oxide form, graphene oxide (GO), which are hydrophilic oxygenated graphene sheets bearing oxygen functional groups on their basal planes and edges, have attracted much attention in recent years [1-3]. GO nanosheets are of particular interest due to their aqueous solubility [1, 2]. GO is very attractive for applications such as energy-related materials, sensors, and bio-applications [4-7]. GO is also a promising candidate for the preparation of paper-like materials [8]. More importantly, GO is considered as a promising precursor for the large-scale production of graphene-based materials owing to its relatively low cost of synthesis [8, 9].

In 1859, Brodie demonstrated the first synthesis method of GO by adding potassium chlorate to a slurry of graphite in fuming nitric acid [10]. Staudenmaier improved this method by adding the chlorate in small portions over the course of the reaction [11]. He also added concentrated sulfuric acid to increase the acidity of the mixture. This slight change in the procedure resulted in an overall increase in the extent of oxidation. Hummers and Offeman introduced in 1958 the most currently used method to prepare GO[12]. They oxidized graphite with $KMnO_4$ and $NaNO_3$ in concentrated H_2SO_4. After oxidizing the bulk graphite, GO sheets are exfoliated from the oxidized bulk via sonication in aqueous solution. All three of these procedures take place over days and involve the generation of the toxic gas(es) NO_2, N_2O_4, and/or ClO_2; the latter also being explosive[13]. In addition, the extensive sonication treatment easily breaks the GO sheets.

Electrochemistry has been previously reported to produce graphene in large quantities [14, 15], but not yet to produce GO that is comparable with the Hummer's process. Herein, we report a single step electrochemical route to exfoliate graphite flakes in the form of GO sheets. The process eliminates the steps that involve toxic or dangerous materials, very easy to operate and scalable.

After few minutes of applying the current on the graphite anode, the colour of the electrolyte changed from very clear transparent to yellowish then to golden, brown, dark brown and finally black (Figure 1). These changes in colour reflect the changes of the GO concentration in the suspension. The GO was well dispersed in the electrolyte, as the suspension was stable for > 5 weeks. The powder collected from the suspension by filtration weighted 0.22g after 6 hours of electrolysis. Also the percentage of the non-exfoliated particles collected after centrifugation to the total loss of the graphite electrode weight was 12-20 wt.%. This low percentage indicates the high efficiency of the electro-oxidative exfoliation.

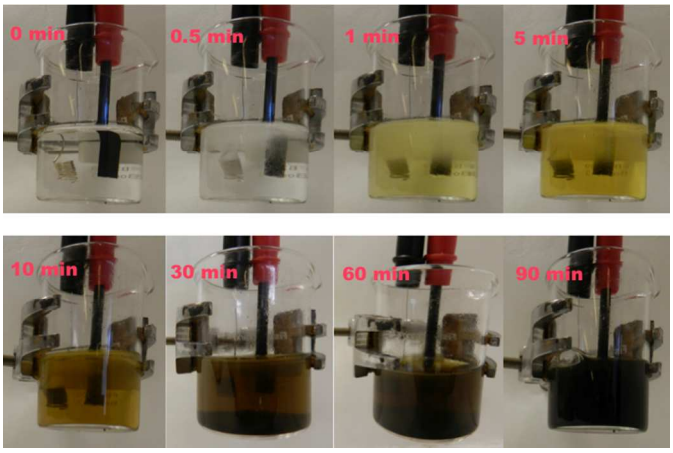

Figure 1: Photograph showing the changes of the solution colour during the electrolysis process.

Figure 2a shows the X-ray diffraction (XRD) patterns of the parent graphite and electrochemically exfoliated GO. The graphite exhibited a single well-defined peak at $2\theta = 26.59^0$, which corresponds to (002) plane. The XRD for the GO has a distinct diffraction peak at $2\theta = 10.24^0$. The figure shows the transformation of the interlayer spacing (d_{002} spacing) from 0.335 to 0.822 nm, which is a clear indication of the complete transformation from graphite to GO [16]. The distance between consecutive carbon layers was increased for GO due to the introduction of oxide functional

ChemComm Accepted Manuscript

groups to the carbon basal plane via the electrochemical oxidation reaction.

The Raman spectra of the electrochemically exfoliated GO and the starting graphite are shown in figure 2b. The GO Raman spectra show G peaks ~1590 cm^{-1} and D peaks ~1350 cm^{-1}. The broadening and the shift of G line to higher frequency and the appearance of broad D line point to intense formation of structural defects and dramatic break up of the original graphite domains, which is in a good agreement with the crystalline changes deduced from the XRD data. The disappearance of the 2D band at ~ 2680 cm^{-1}, which is typical for multilayer graphene structures of the graphite, also confirms the lattice distortions [17]. This high density of defects in GO is due to the large abundance of oxygenated functional groups that disrupt the planar sp^2 structure [17].

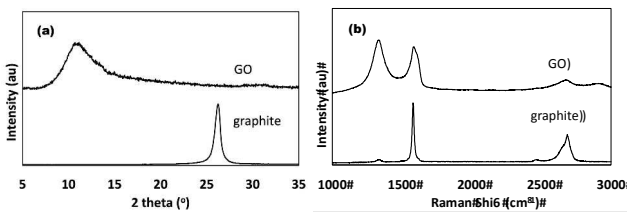

Figure 2: **(a)** XRD pattern of the produced GO powder and the graphite used as a raw material, (b) typical Raman spectrum of the initial graphite and the produced GO

The thickness of the exfoliated GO was examined using atomic force microscope (AFM). The height profile of the AFM image (figure 3) indicates that the thickness of the obtained GO sheet is about 1.1 nm, suggesting the successful exfoliation of graphite down to individual GO sheets was indeed achieved under the electro-oxidative conditions [18, 19]. Although, a pristine graphene sheet is atomically flat with a well-known thickness of 0.34 nm, GO is expected to be thicker owing to the presence of functionalized oxygen and hydrocarbon groups attached above and below the original graphene plane [9, 18]. These functional groups disrupts the original conjugation and introduces lattice defects to result in folds and distortions on the sheets, which explains also the slightly thicker layers than the interlayer spaces measured by the XRD.

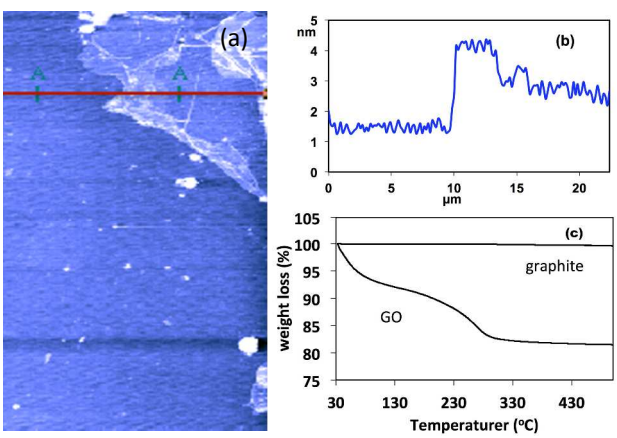

Figure 3: (a) Tapping mode AFM image and (b) height profile shown mono and bilayer GO, (c) TGA curve of the produced GO as compared to the graphite feed materials**.**

Figure 3c displays the TGA curves for samples exfoliated via the electro-oxidative process measured between room temperature and 800 °C in N_2. The TGA curve exhibits two weight losses: from room temperature to 110 °C and from 275 to 400 °C. The lower temperature mass loss of 5.71% is due water molecules absorbed into the reduced GO bulk material, the following loss of 12.4% decrease stands for elimination of remaining functional groups, further decomposition take place up to 800°C [20, 21]. This curve is in agreement with the TGA curve recorded for GO produced by the Hummer process [20, 22].

X-ray photoelectron spectroscopy (XPS) was used to establish the composition of the exfoliated products after electro-oxidation and multiple washing. As shown in the XPS survey scan in Figure 4, the C_{1s} band can be fitted to seven deconvulated components. Components located at 284.5 and 285.0eV can be assigned to the non-oxygenated ring carbon C-C/C-H (sp^3), and C=C (sp^2), respectively. The binding energies of components at 286.4eV, 287.0, 288eV and 289 would be consistent with C-OH (hydroxyl), epoxy, carbonyl and carboxyl / ester respectively [9, 23, 24]. These results showed clearly that the electro-oxidative process has introduced oxygenated functional groups into the graphene surface. However, the carbon/oxygen ratio is 7.6 which implies a significantly oxygen deficient GO surface compared to GO prepared by the Hummer process which typical has a carbon/oxygen = 2.0. This ratio is also lower than that reported for reduced graphene oxide, which makes the electrochemically produced GO a suitable precursor for the production of graphene and many other applications.

However, for some other applications, more functionalized group and in general higher oxygen content is needed. It was found to be possible to tune the current process for further oxidation of the graphite materials. Nitric acid was added to the solution in a concentration of 0.2M. The total oxygen content increased to give a C/O ratio of about 4 as can be calculated from the XPS analysis. High-resolution scan of the C1 peak showed also increase in the intensity of the hydroxyl, epoxy, carbonyl and carboxyl / ester groups peaks. In addition to these groups, the survey scan detected a new peak at 400eV corresponding to nitrogen (see supplementary information).

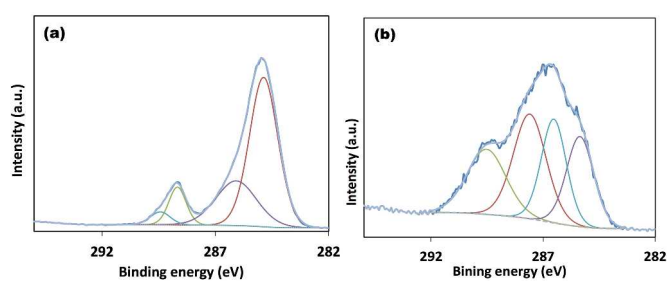

Figure 4: (a) High resolution XPS of the C1s spectra of the GO produced from the buffer solution, (b) the C1s spectra after adding HNO_3

To understand the reactions mechanism, samples were taken of the electrolyte at different intervals and studied by SEM and TEM. Figure 5 shows the structures found at different stages of the process. At the first stag of the process, round shape 20-100 nm particles (figure 5a) and nanoribbons (figure 5b) resulted from the anodic process. Similar particles have been reported before as a corrosion product of graphite in aqueous solutions [25], suggesting that the first stage of the process is mainly the reaction of graphite with hydrogen

ChemComm Accepted Manuscript

This journal is © The Royal Society of Chemistry 2012

radical at the edges of the graphene plans forming water-soluble hydrocarbon/carbon crystals. In the later stages, when the intercalation starts to take place on the defects created by the corrosion reaction, sheets several micron in diameter were observed. These intercalations weaken the bond between the graphene sheets and increase the interlayer distance, which facilitated the corrosion reaction further. The gasses product of the corrosion reaction and the gases produced by the dissociation of the intercalation compounds pushes the graphene sheets further and lead to the exfoliation.

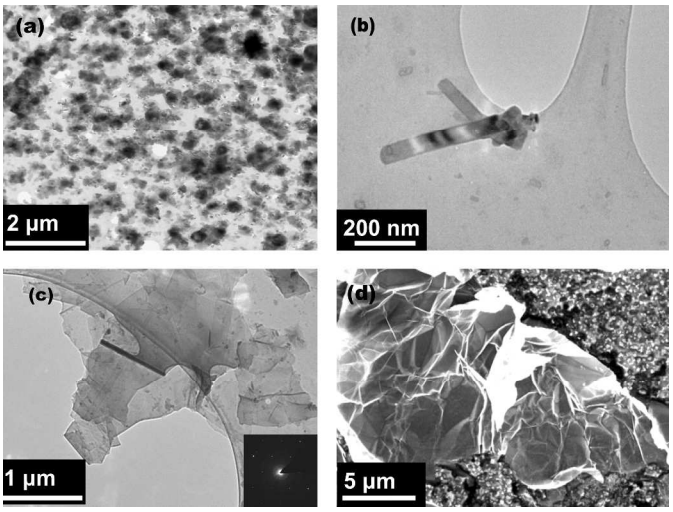

Figure 5: (a) TEM image of the hydrocarbon nanoparticles produced at the first stage of electrolysis, (b) nanoribbons resulted also at early stage of electrolysis (c) TEM image of typical GO sheet resulted after 5 hours of electrolysis (note the aggregation of the flakes during removing the water from the suspension), (inside) diffraction pattern of the GO sheet in c, (d) Typical SEM image of GO produced from puffer solution after 5 hours of electrolysis.

Conclusions

We have demonstrated a scalable electrochemical method to produce GO flakes from graphite. By using graphite as an anode in electrochemical cell contains 0.2 M sodium citrate, graphite oxidation and exfoliation takes place simultaneously resulting in a GO flakes with 7.6 carbon/oxygen ratio. We have shown also the possibility of controlling the oxidation level by controlling the composition of the electrolyte. Studying the reaction mechanism revealed that the process started by forming 20-100 nm particles and nanoribbons graphite with hydrogen radical at the edges of the graphene plans. The process proceeds much faster after that with the anion intercalating with graphite and weaken the bond between the graphene sheets. Our method is considerably quicker and more environmentally friendly than the traditional Hummers' Rout and we believe it will greatly facilitate the large-scale production of GO.

Notes and references

[a] School of Materials, University of Manchester.
[b] School of Chemistry, University of Manchester.

Electronic Supplementary Information (ESI) available: [experimental details, XPS, more SEM images, AFM]. See DOI: 10.1039/c000000x

1. H. He, J. Klinowski, M. Forster and A. Lerf, *Chemical Physics Letters*, 1998, **287**, 53-56.
2. G. I. Titelman, V. Gelman, S. Bron, R. L. Khalfin, Y. Cohen and H. Bianco-Peled, *Carbon*, 2005, **43**, 641-649.
3. D. A. Dikin, S. Stankovich, E. J. Zimney, R. D. Piner, G. H. B. Dommett, G. Evmenenko, S. T. Nguyen and R. S. Ruoff, *Nature*, 2007, **448**, 457-460.
4. S. Park, N. Mohanty, J. W. Suk, A. Nagaraja, J. H. An, R. D. Piner, W. W. Cai, D. R. Dreyer, V. Berry and R. S. Ruoff, *Advanced Materials*, 2010, **22**, 1736-+.
5. J. Wu, W. Pisula and K. M√°llen, *Chemical Reviews*, 2007, **107**, 718-747.
6. M. D. Stoller, S. Park, Y. Zhu, J. An and R. S. Ruoff, *Nano Letters*, 2008, **8**, 3498-3502.
7. D. Chen, H. Feng and J. Li, *Chemical Reviews*, 2012, **112**, 6027-6053.
8. C. Chen, Q.-H. Yang, Y. Yang, W. Lv, Y. Wen, P.-X. Hou, M. Wang and H.-M. Cheng, *Advanced Materials*, 2009, **21**, 3007-3011.
9. S. Stankovich, D. A. Dikin, R. D. Piner, K. A. Kohlhaas, A. Kleinhammes, Y. Jia, Y. Wu, S. T. Nguyen and R. S. Ruoff, *Carbon*, 2007, **45**, 1558-1565.
10. B. C. Brodie, *Philosophical Transactions of the Royal Society of London*, 1859, **149**, 249-259.
11. L. Staudenmaier, *Berichte der deutschen chemischen Gesellschaft*, 1898, **31**, 1481-1487.
12. W. S. Hummers and R. E. Offeman, *J. Am. Chem. Soc.*, 1958, **80**, 1339-1339.
13. D. R. Dreyer, S. Park, C. W. Bielawski and R. S. Ruoff, *Chemical Society Reviews*, 2010, **39**, 228-240.
14. A. M. Abdelkader, I. A. Kinloch and R. A. W. Dryfe, *ACS Applied Materials and Interfaces*, 2014, **6**, 1632-1639.
15. A. J. Cooper, N. R. Wilson, I. A. Kinloch and R. A. W. Dryfe, *Carbon*, 2014, **66**, 340-350.
16. D. C. Marcano, D. V. Kosynkin, J. M. Berlin, A. Sinitskii, Z. Sun, A. Slesarev, L. B. Alemany, W. Lu and J. M. Tour, *ACS Nano*, 2010, **4**, 4806-4814.
17. K. N. Kudin, B. Ozbas, H. C. Schniepp, R. K. Prud'homme, I. A. Aksay and R. Car, *Nano Letters*, 2007, **8**, 36-41.
18. J. I. Paredes, S. Villar-Rodil, P. Sol√≠s-Fern√°ndez, A. Mart√≠nez-Alonso and J. M. D. Tasc√≥n, *Langmuir*, 2009, **25**, 5957-5968.
19. D. Li, M. B. Muller, S. Gilje, R. B. Kaner and G. G. Wallace, *Nat Nano*, 2008, **3**, 101-105.
20. K. Zhang, L. L. Zhang, X. S. Zhao and J. Wu, *Chemistry of Materials*, 2010, **22**, 1392-1401.
21. J. Shen, Y. Hu, C. Li, C. Qin and M. Ye, *Small*, 2009, **5**, 82-85.
22. M. J. McAllister, J.-L. Li, D. H. Adamson, H. C. Schniepp, A. A. Abdala, J. Liu, M. Herrera-Alonso, D. L. Milius, R. Car, R. K. Prud'homme and I. A. Aksay, *Chemistry of Materials*, 2007, **19**, 4396-4404.
23. S. Dubin, S. Gilje, K. Wang, V. C. Tung, K. Cha, A. S. Hall, J. Farrar, R. Varshneya, Y. Yang and R. B. Kaner, *ACS Nano*, 2010, **4**, 3845-3852.
24. S. Park, J. An, J. R. Potts, A. Velamakanni, S. Murali and R. S. Ruoff, *Carbon*, 2011, **49**, 3019-3023.
25. J. Lu, J. X. Yang, J. Wang, A. Lim, S. Wang and K. P. Loh, *ACS Nano*, 2009, **3**, 2367-2375.

ChemComm Accepted Manuscript